VALIDATION OF POINT SCATTERER PHASE STATISTICS IN MULTI-PASS INSAR

Gini Ketelaar, Petar Marinkovic and Ramon Hanssen

Delft Institute of Earth Observation and Space Systems; Delft University of Technology
Kluyverweg 1, 2629 HS Delft, The Netherlands
V.B.H.Ketelaar@lr.tudelft.nl

ABSTRACT

In radar images, point scatterers provide reflections that can often be attributed to a single physical object, usually smaller than the resolution cell size. Stable point scatterers with high backscatter coefficients through time (mainly 'man-made features') are potential targets for InSAR deformation analysis.
A-priori knowledge about the observation statistics of InSAR point scatterer measurements is necessary to give an independent quality description of the estimated (deformation) parameters. Using the Signal-to-Noise Ratio (SCR) from SAR images an a-priori estimate of the phase variance can be obtained.
A controlled corner reflector experiment has been set up with leveling as an independent validation technique. In the period from March 2003 to June 2004 the movements of five corner reflectors in the area near Delft University of Technology have been monitored using leveling and repeat-pass InSAR (ERS-2 and Envisat).
Double-difference observations, the first observations that bear interpretable information, are used for comparing the InSAR and leveling measurements. The stochastic model is set up as a variance-covariance matrix, estimating a-posteriori variance factors for the observation groups leveling, ERS-2 and Envisat. From the results it can be concluded that the a-priori phase variance based on SCR for the corner reflectors (σ $\sim$0.4mm) is significantly overestimated. The estimated a-posteriori InSAR phase standard deviation is 3.1 mm for Envisat and 3.9 mm for ERS-2 (mm, vertical).

1. INTRODUCTION

The Persistent Scatterer (PS) InSAR technique [1] uses observations from selected stable point scatterers having high backscatter coefficients through time. These point scatterers provide reflections that can often be attributed to a single physical object ('man-made feature'), usually smaller than the resolution cell size.

PS's serve as measurement points for deformation analysis. Using InSAR observations, the first information-bearing variate is the phase difference between two interferometric resolution cells: the double- difference phase observation [2]. Besides deformation information, this wrapped observable also contains contributions due to (residual) topography, orbital errors and atmospheric signal.

Several techniques are currently used to estimate these parameters. One of these techniques is based on searching the solution space optimizing the single-pixel multi-interferogram complex coherence based on the phase residuals through time [3]. Another approach is presented in [4], constructing a mathematical model, taking the stochastic nature of the observables into account. The integer phase ambiguities are estimated using the LAMBDA method [5], treating the ambiguities as stochastic, not deterministic.

As the application of the PS-InSAR technique is expanding towards decorrelated areas with low PS density and a small deformation signal, the quality description of the estimated (deformation) parameters becomes more and more important. As the precision of the phase observables directly influences the parameter estimation, it is important to properly define their variance-covariance matrix. The probability density function of distributed scatterers is well known [6], but determining the variance of a point scatterer phase observation is not trivial. Contrary to other geodetic measurement techniques, the variance of the observable is not very well known a-priori. The reason for this is that precision of a double-difference point scatterer phase observation depends both on the device

Proc. of the 2004 Envisat & ERS Symposium, Salzburg, Austria
6-10 September 2004 (ESA SP-572, April 2005)

measurement precision and the physical properties of the point scatterer and its surroundings. These two effects cannot easily be separated.

As shown in [3] there is a relation between the coherence and the variance of the phase observable of a point scatterer. However, the point scatterer coherence is based on the residuals of the PS-InSAR parameter estimation, and therefore these parameters have to be resolved first. The consequence of this is that model imperfections are mixed with the point scatterer observable variance. To be able to give an independent quality description of both the stochastic model of the observables and the estimated parameters, they have to be set up separately, forming together an integrated mathematical model on which adjustment and testing theory can be applied. Here we focus on the stochastic model of the PS-InSAR double-difference phase observations.

Besides the measurement device precision, the point scatterer phase observation precision is dependent on its physical properties and the surroundings. The physical properties determine the strength and the pattern of the reflection. The surroundings can be interpreted as an amount of scatterers, which all have their own sinc pattern in space. These are overlaying the point scatterer reflection pattern, introducing noise on the point scatterer phase observation. Considering the point scatterer as a signal plus circular random gaussian noise, it has been shown that the point scatterer phase variance can be estimated using the Signal-to-Clutter Ratio (SCR) [9]. This estimate is unbiased for a low phase variance (≤ 0.25 rad) and assumes ergodicity of the surroundings.

In this research, the SCR is used for obtaining an a-priori estimate for the phase variance. This means that one point scatterer may have different variances through time, depending on the surroundings. As the SCR is a spatial estimate from the SAR image, parameter estimation is not needed to obtain the phase variance. In this way the stochastic model is set up independently from the functional model. To verify this approach, the InSAR phase observations of the Delft corner reflector experiment [7] are used. Five corner reflectors have been deployed in the fields of Delft Technical University since March 2003. Each satellite pass, a precise leveling was carried out, to validate the phase history of the corner reflectors. The InSAR and leveling time series of these five point scatterers are used to validate the stochastic model of the InSAR phase observations. A corner reflector experiment that compares InSAR with GPS measurements is described in [8].

This paper is split up in the following two sections:

- Point scatterer theory and SCR estimation of the five corner reflectors through time, checking their dependence on temporal baseline and Doppler shift.
- A-posteriori precision estimation for leveling, ERS-2 and Envisat double-difference observations, starting from the a-priori variance-covariance matrix based on SCR.

2. PHASE VARIANCE ESTIMATION BASED ON SCR

2.1. Point scatterer

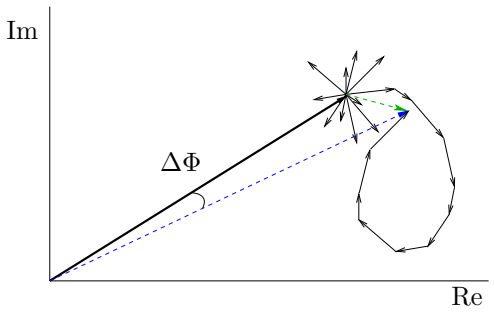

Figure 1. Point scatterer

The Signal-to-Clutter Ratio (SCR) is used for estimating the phase variance of a point scatterer, based on its physical properties. A point scatterer is considered as a deterministic signal s, disturbed by clutter $\underline{c}$: random circular gaussian noise of distributed scatterers in the surroundings (Fig. 1). The underlining of a variable indicates its stochastic nature. The complex SLC SAR observable of a point scatterer $\underline{z}$ is defined as

$$\underline{z} = s + \underline{c} = a + ib + \underline{u} + i\underline{v} = (a + \underline{u}) + i(b + \underline{v}) \quad (1)$$

$$u, v \sim N(0, \sigma) \quad \mathrm{Re(z)} \sim \mathrm{N(a, \sigma)} \quad \mathrm{Im(z)} \sim \mathrm{N(b, \sigma)} \quad (2)$$

where σ is the clutter standard deviation for Re and Im. According to this definition, the phase residual

$$\Delta\underline{\Phi} = \arctan \frac{b + \underline{v}}{a + \underline{u}} - \arctan \frac{b}{a} \quad (3)$$

is a nonlinear function of normal distributed variables. Therefore phase residuals are often not normally distributed. Simulations have been performed to verify the normality of the phase residuals of a point scatterer, using a large number of samples.

A Goodness-of-Fit test indicates whether a dataset consisting of a number of realizations stems from a certain distribution. The Kolmogorov-Smirnov test is such a Goodness-of-Fit test. It's teststatistic is defined as the maximum absolute difference

between the cumulative distribution of the dataset and the cumulative hypothesized distribution, which is in this case the normal distribution. The Lilliefors Goodness-of-Fit test defines its teststatistic similar to the Kolmogorov-Smirnov teststatistic, but also estimates the parameters of the normal distribution from the dataset.

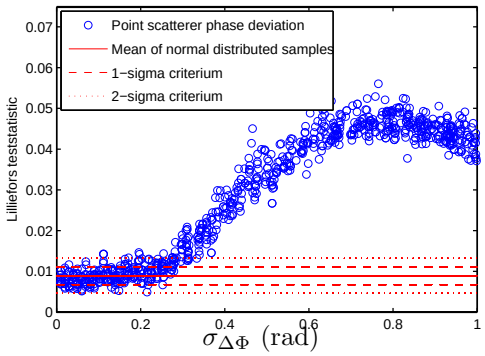

Figure 2. Goodness-of-Fit for normal distribution of points scatterer phase residuals.

The values of the Lilliefors teststatistic have been computed for both the point scatterer phase residuals and an equal number of independent samples from the normal distribution, see Fig. 2. From the deviation of the reference normal distribution, indicated by the horizontal lines in Fig. 2, it can be concluded that the phase residuals are only approximately normally distributed if the phase standard deviation is lower than 0.25 rad (≈2.2mm).

Methods to estimate the phase variance are the dispersion index D_a [1] and SCR [9]. Both methods start to develop a bias in the phase variance estimate compared to the phase variance based on RMS at approximately the same point where the phase residuals cannot be assumed to be normally distributed anymore. The question raises if only targets with a SCR higher than 8 can be considered as point scatterers, or if the useful information in targets with a lower SCR can be used, using different statistics to describe their variance. However, this study focuses on corner reflectors that have a SCR higher than 100. It should therefore be possible to obtain an unbiased estimate of their phase variance using SCR.

2.2. Signal-to-Clutter Ratio

Both D_a and SCR can be used to detect Persistent Scatterer candidates and both can be used to estimate the phase variance. D_a is a single-pixel through time estimate, whereas SCR is a spatial estimate. As the point scatterer phase variance is mainly determined by the possibly changing scattering characteristics of its surroundings, we chose to base the estimate of the phase variance on SCR.

SCR and the phase variance estimate [9] are defined as

$$SCR = \frac{s^2}{c^2} \tag{4}$$

$$\sigma_\phi^2 = \frac{1}{2SCR}(\text{rad}). \tag{5}$$

SCR estimation has been performed for all five corner reflectors. The signal amplitude value s is the maximum amplitude value of the oversampled sinc pattern (factor 16) of the corner reflector.

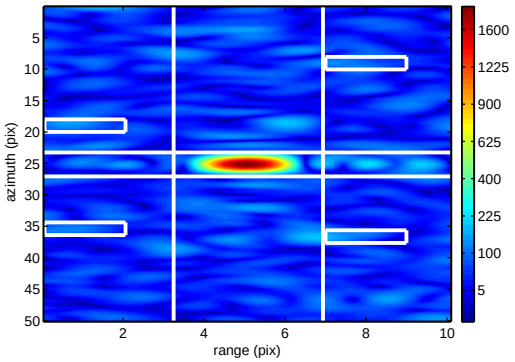

Figure 3. Windows used for SCR estimation with maximum clutter samples (amplitude values).

For estimating the clutter, the boundaries of the sinc pattern of the corner reflectors were traced using an edge detector. This resulted in four areas around the corner reflector not affected by the point scatterer signal, see Fig. 3. There are several ways to estimate the clutter from these four windows. The most commonly used method is searching the four areas with a small sampling window and detecting the minimal clutter amplitude. However, it could be argued that it is better to detect the maximum clutter amplitude or using the average over the full clutter area. The objective is to estimate the clutter at the corner reflector position (resolution cell). Clutter can be regarded as a collection of distributed scatterers which have their own (smaller) sinc pattern in space. As the SAR data is sampled in range and azimuth direction, the side lobes are only propagating in range and azimuth direction. One would like to take samples within the corner reflector azimuth and range boundaries as well, but that is not possible as those samples would be highly disturbed by the corner reflector's own sinc pattern. As a result of this, the sampling areas

are restricted outside the corner reflector's azimuth and range boundaries. When estimating clutter in these regions, there is no reason to assume that the 'true' clutter of the point scatterer's resolution cell is equivalent to the minimum of the estimation regions. In fact, it is certain that this will result in a phase variance that is too small. Therefore, to obtain conservative estimates of the phase precision, we use the mean of the maximum of the clutter estimates in the four sampling areas.

The clutter estimate is only unbiased if the ergodicity assumption holds. As the corner reflectors have been placed in a large homogeneous field, 200 meter apart, this assumption is reasonable.

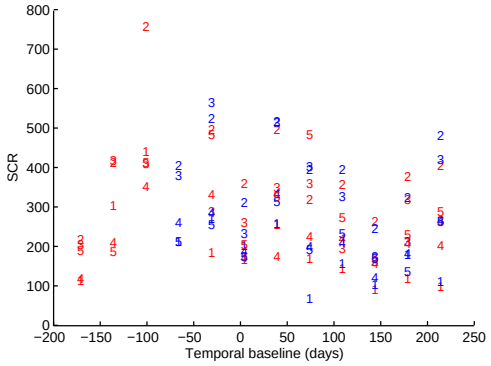

Figure 4. SCR values for corner reflectors 1-5 through time, for ERS-2 (red) and Envisat (blue).

Fig. 4 shows the SCR for the five corner reflectors for all available acquisitions. There is a slight seasonal trend visible, which may be caused by clutter changes due to vegetation changes in the surrounding field or by thermal effects. The magnitude of the SCR values is of the same order for ERS-2 and Envisat. As SCR should be purely depending on the physical properties of the scatterer, it should be sensor independent, what is confirmed by Fig. 4. The order of the corner reflectors in terms of SCR magnitude changes through time, but in general the corner reflectors 2, 3, and 5 have a larger SCR than 1 and 4. Especially after the damage of corner reflector 1 (B^T=-70 days), it is in the lower SCR regions. Changes in SCR may be caused by alignment changes towards the satellite or clutter changes.

Note that it is not necessary to calibrate the SAR amplitudes of the corner reflectors for the estimation of the phase variance based on SCR. The calibration causes the amplitudes to be multiplied by a certain factor, depending on viewing geometry and sensor characteristics. The viewing geometry dependent factor is slowly changing from near to far range and can be considered equal for the corner reflector signal and the clutter in its direct surroundings. The replica pulse power correction results in one factor for the full scene. And finally, regarding the powerloss, distributed and point scatterers within an area of the radar footprint (around 5 by 5 km in azimuth and range) are affected in the same way as they cannot be distinguished within the full reflected signal. This means, that for calibration the signal and the clutter amplitude would be multiplied by the same factor, that would cancel out in SCR.

2.3. Corner reflector SCR estimates

For all five corner reflectors SCR has been calculated for the ERS-2 and Envisat acquisitions in the period March 2003 - Jun 2004. Fig. 5 and 6 show clutter and signal amplitudes and the estimated phase standard deviations σ_ϕ in time.

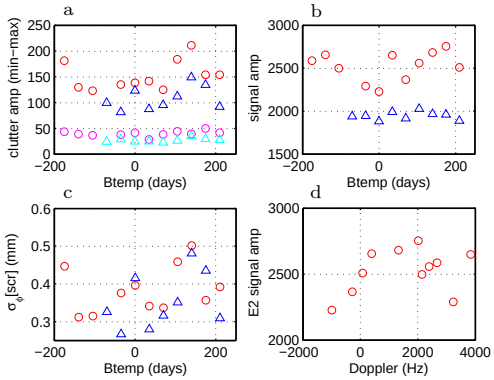

Figure 5. CR3: (a) minimum and maximum clutter amplitudes against temporal baseline, (b) signal amplitudes in time (c) σ_ϕ based on SCR in time (d) signal amplitudes against Doppler for ERS-2. ERS-2: red circles, Envisat: blue triangles.

Regarding the clutter, both minimum and maximum have been plotted. The maximum clutter appears to have a higher variation than the minimum clutter. This might be due to fact that maximum clutter corresponds to incidental clutter scatterers, whereas the minimum clutter can be regarded as background noise. Unlike the signal amplitudes, the clutter seems to follow a slight temporal trend, but this is not evident.

A clear offset is visible between the ERS-2 (red circles) and Envisat (blue triangles) signal amplitudes. This is caused by the difference between the sensors, but it may also depend on the alignment of the corner reflector towards the satellite (look angle). As the ERS-2 SAR images have large Doppler shifts,

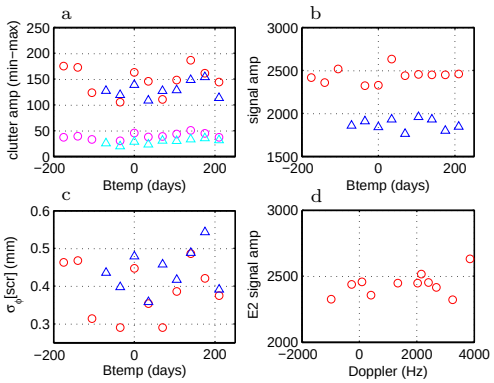

Figure 6. CR5: (a) minimum and maximum clutter amplitudes against temporal baseline, (b) signal amplitudes in time (c) σ_ϕ based on SCR in time (d) signal amplitudes against Doppler for ERS-2. ERS-2: red circles, Envisat: blue triangles.

which influences the viewing geometry in azimuth direction, the Doppler shifts have been plotted against the SAR amplitudes. The results for this one year time span do not indicate a dependency of the signal amplitude on Doppler frequency shift.

Note that also the Envisat clutter amplitudes are generally below those of ERS-2. The offset decreases with decreasing amplitude and it is therefore likely that a multiplication factor connects the ERS-2 and Envisat amplitudes, like in SAR calibration. When looking at the estimates of the phase standard deviation based on SCR, ERS-2 and Envisat are at the same level. ERS-2 and Envisat signal and clutter differences seem to cancel out in the SCR computation.

The estimated phase standard deviations do not seem to vary significantly in time and the values coincide for ERS-2 and Envisat. This would mean, that estimation the SCR's of the corner reflectors in a single SAR image is enough to obtain a-priori phase variances. However, it has to be noted that the time dependence of the phase variance is likely to be determined by the SCR of the point scatterer relative to the changes in the direct surroundings. In case the phase variance cannot be considered as a constant value, it's time dependency has to be accounted for in the a-priori variance-covariance matrix (vc matrix) of the InSAR observations, as it influences the parameters to be estimated.

2.4. Statistics of wrapped double-difference distributed phases.

For comparing the InSAR double-differences with the leveling double-differences, the InSAR double-differences are unwrapped to the closest leveling double-difference. The misclosures are therefore limited to half a cycle. This paragraph deduces the maximum standard deviation of phase double-differences to be expected in case the corner reflectors would statistically behave like distributed in stead of point scatterers.

InSAR phase measurements in this paper are expressed in mm along the vertical. This means that in case of ERS-2, having an effective wavelength of 28.3 mm, the InSAR phase measurement range is

$$[-\frac{\lambda}{4\cos(\theta_{\text{inc}})}, \frac{\lambda}{4\cos(\theta_{\text{inc}})}] = [-15.4, +15.4]\text{mm}. \quad (6)$$

Interferometric phase measurements, with W as the wrapping operator, are defined as:

$$\varphi_{cr}^{m-s} = W\{(\phi_{cr}^{m} - \phi_{cr}^{s})\}. \quad (7)$$

Double-differences are defined as the interferometric phase measurements between two resolution cells or PS's at a certain distance:

$$\varphi_{cr_a-cr_b}^{t_m-t_s} = W\{(W\{(\phi_{cr_a}^{t_m} - \phi_{cr_a}^{t_s})\} - W\{(\phi_{cr_b}^{t_m} - \phi_{cr_b}^{t_s})\})\}. \quad (8)$$

For distributed scatterers, the phase is uniformly distributed. The range of the uniform distribution is equal to $[-\frac{\lambda}{4\cos(\theta_{\text{inc}})}, +\frac{\lambda}{4\cos(\theta_{\text{inc}})}]$, expressed in mm along the vertical. Fig. 7 shows the phase distribution of InSAR phase measurements and the double-differences, without and with applying the wrapping operator. Without applying the wrapping operator, the distribution of double-differences is a double convolution of the uniform distribution. However, when applying the wrapping operator, SAR, InSAR and double-difference phase observations have the same uniform distribution for distributed scatterers.

For point scatterers with a low dispersion index, phases are approximately normally distributed. In this case the variances of the double-difference phase measurements can be calculated using the propagation law, assuming master, slave and the corner reflectors to be uncorrelated:

$$\sigma^2_{\varphi_{cr_a-cr_b}^{t_m-t_s}} = \sigma^2_{\phi_{cr_a}^{t_m}} + \sigma^2_{\phi_{cr_a}^{t_s}} + \sigma^2_{\phi_{cr_b}^{t_m}} + \sigma^2_{\phi_{cr_b}^{t_s}}. \quad (9)$$

The phase variances needed to calculate the double-difference variance are estimated using the SCR of each corner reflector in each SAR image.

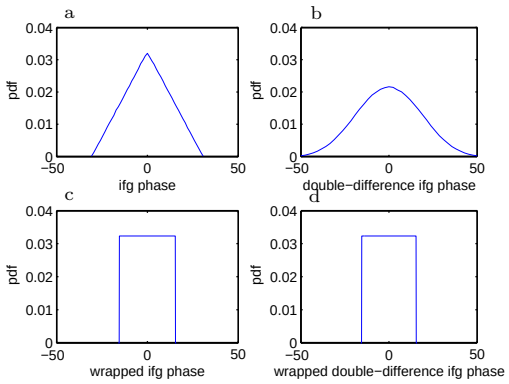

Figure 7. PDF of (a) interferometric phases of distributed scatterers, (b) double-difference interferometric phases of distributed scatterers, (c) and (d) wrapped interferometric phases of (double-difference) distributed scatterers. Phase units are mm along the vertical.

To judge the level of significance of the estimated InSAR double-difference precision of the corner reflectors using leveling as validation technique, they are compared to the maximum standard deviation of double-differences of distributed scatterers. This standard deviation follows from the uniform distribution, depending on the effective wavelength:

$$\sigma^2_{\varphi^{m-s}_{a-b}} = (\frac{\lambda}{4\cos(\theta_{\text{inc}})})^2/3. \qquad (10)$$

For ERS-2 and Envisat this would result in a maximum double-difference standard deviation of 8.8 mm for the InSAR-leveling comparison.

3. A-POSTERIORI PRECISION ESTIMATION.

This section describes the a-posteriori precision estimation of InSAR double-differences using independent leveling measurements and Variance Component Estimation (VCE). To validate the phase history of the corner reflectors, it is compared with measurements from the independent leveling technique. First, the results of the performed levelings will be shown. Consequently, the leveling and InSAR double-differences are graphically compared. Finally, the a-posteriori phase variances for ERS-2 and Envisat are estimated using VCE and a mathematical model consisting of a functional model and an a-priori stochastic model.

3.1. Leveling measurements

At the time of each satellite pass, a leveling of the five corner reflectors was performed. The leveling network has been designed containing redundancy, which makes it possible to detect erroneous height difference measurements. The leveling network contains two benchmarks founded on a stable subsurface layer. Through time, the height difference between these benchmarks varies at most 0.5 mm and can therefore be considered as stable. However, the corner reflectors have been established in a shallow subsurface layer and appear to be moving 1–2 cm seasonally. As the leveling height measurement precision is around 0.3–1.5 mm, this seasonal movement is significant and it should be possible to detect it using InSAR.

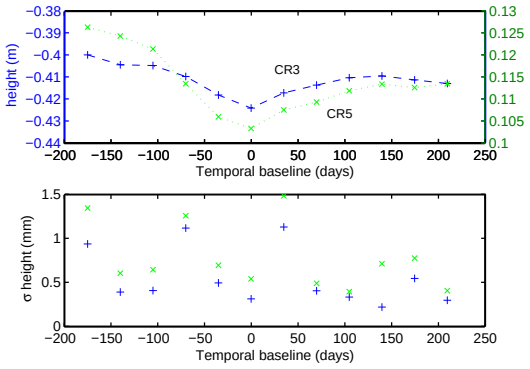

Figure 8. Leveling heights and standard deviation for CR3 and CR5.

Fig. 8 shows the estimated leveling heights and their precision for corner reflectors 3 and 5. They result from the adjustment and testing procedure of the leveling network height difference observations. Erroneous observations were traced using datasnooping and removed. The seasonal trend is visible. Time $t = 0$ corresponds with September 2003; during summer the corner reflectors subsided whereas in autumn the uplift started. Possibly precipitation expanded the subsurface layer. The height standard deviation varies between 0.3 and 1.5 mm, depending on weather circumstances and leveling network construction.

The adjustment and testing procedure results in a vc matrix for the estimated heights. The covariances between the corner reflector heights depend on the network design. This vc matrix, containing both variances and covariances is used to create the vc matrix of the leveling double-differences, using the propagation law. The vc matrix of the leveling double-differences is then used in the a-priori vc matrix for the InSAR-leveling double-differences comparison.

3.2. InSAR-leveling double-differences

As mentioned in the introduction, the double-difference phase observation is the first variate, that bears interpretable information. Therefore the InSAR-leveling comparison is based on these double-differences. One master has been chosen for both ERS-2 and Envisat (September 2003), and all spatial differences have been referenced to corner reflector 2. As the maximum distance to the reference corner reflector is 600 meters, atmospheric effects are assumed to be canceled in the spatial difference. To be able to compare InSAR and leveling double-differences, the InSAR phase double-differences have been transformed to mm along the vertical, using the incidence angle.

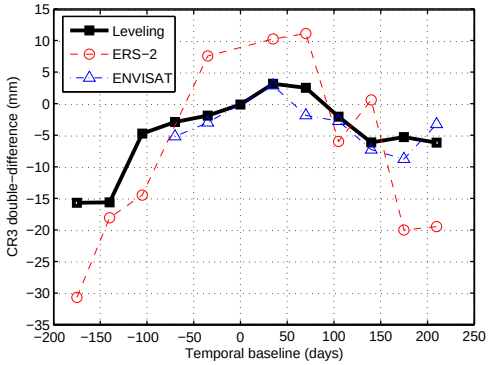

Figure 9. Time series leveling, ERS-2 and Envisat double-differences for CR 3.

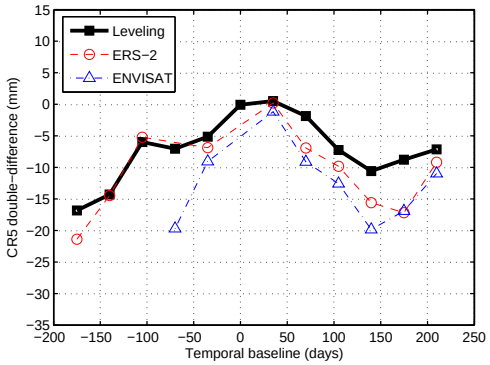

Figure 10. Time series leveling, ERS-2 and Envisat double-differences for CR 5.

Fig. 9 and 10 show the leveling, ERS-2 and Envisat double-difference time series for two of the corner reflectors: 3 and 5. For corner reflector 3, the Envisat double-differences match the leveling double-differences closely, whereas ERS-2 exhibits high deviations. For corner reflector 5, there seems to be a deviating trend in time of the InSAR double-differences from the leveling double-differences.

The cause of the ERS-2 deviations from the leveling may be found in the interferometric processing chain. We note that our implementation to compensate the influence of the position of the point scatterer within the resolution cell on the phase measurement needs to be improved for large baselines and large Doppler shifts. The deviating behavior of both Envisat and ERS-2 from the leveling double-diffferences may be caused by physical changes of the corner reflector in time. The corner reflector's blades for instance may be sagging in time, increasing the InSAR measurements systematically in time. Whereas the apex, to which the leveling measurements are referenced, stays the same.

3.3. Stochastic model

To apply the Delft adjustment and testing theory a functional model, describing the relation between observations and unknown parameters, and a stochastic model has to be set up. The stochastic model is described by the vc matrix of the observations Q_y, in this case the InSAR and leveling double-differences. An a-priori vc matrix is constructed using the vc matrix of the leveling heights from the leveling network adjustment and the variances based on SCR of the InSAR double differences as described in Eq. 9. The corner reflector's interferometric phase measurements are assumed to be uncorrelated in time and space.

The a-posteriori precision estimation for InSAR and leveling double-differences is performed applying Variance Component Estimation [10] using the disjunctive group model. The observables are partitioned into 3 uncorrelated groups: leveling, ERS-2 and Envisat. The dispersion of each group is described by a vc matrix Q_k with an unknown variance factor σ_k^2:

$$Q_y = \sum_{k=1}^{3} \sigma_k^2 Q_k = \begin{bmatrix} \sigma_{\mathrm{Lev}}^2 Q_{\mathrm{Lev}} & 0 & 0 \\ 0 & \sigma_{\mathrm{E2}}^2 Q_{\mathrm{E2}} & 0 \\ 0 & 0 & \sigma_{\mathrm{ES}}^2 Q_{\mathrm{ES}} \end{bmatrix} \tag{11}$$

where

Q_y	vc matrix of observables,
σ_k^2	variance factor for observable group k,
Q_k	vc matrix of observable group k,
Lev	leveling,
E2	ERS-2,
ES	Envisat.

Using the Delft adjustment and testing theory [11] [12], unbiased estimates for the variance factors can be obtained solving the following set of equations:

$$\underline{\hat{\sigma}} = \begin{bmatrix} \hat{\sigma}^2_{\mathrm{Lev}} \\ \hat{\sigma}^2_{\mathrm{E2}} \\ \hat{\sigma}^2_{\mathrm{ES}} \end{bmatrix} = N^{-1}\underline{l} \tag{12}$$

$$N_{kl} = \mathrm{trace}(\mathrm{Q_y^{-1}P_A^{\perp}Q_kQ_y^{-1}P_A^{\perp}Q_l}) \tag{13}$$

$$\underline{l}_k = \underline{y}^* Q_y^{-1} P_A^{\perp} Q_k Q_y^{-1} P_A^{\perp} \underline{y}. \tag{14}$$

With $P_A^{\perp}$ the orthogonal projector:

$$\underline{\hat{e}} = P_A^{\perp}\underline{y} \tag{15}$$

where

Q_y	vc matrix of observables,
Q_k	vc matrix of observable group k,
σ_k^2	variance factor for observable group k,
$\hat{\sigma}_k^2$	variance factor estimate for group k,
$\underline{y}$	vector of observables,
$P_A^{\perp}$	orthogonal projector,
$\underline{\hat{e}}$	vector of least squares residuals.

Application of the disjunctive group model to the leveling and InSAR double-differences revealed an overestimation of the precision of the InSAR double-differences. Fig. 5 and 6 show an average standard deviation of 0.4 mm for a single SAR phase observation (mm, vertical), which propagates into 0.8 mm for an InSAR double-difference observation. From Fig. 9 and 10 you can deduce that the InSAR double-differences deviate more from the leveling double-differences, even when taking a standard deviation of leveling double-differences of 1 mm into account. Therefore first the vc matrix has been split up in a known leveling part and an unknown InSAR part. In this step only two variance factors for respectively ERS-2 and Envisat are estimated. Afterwards, a single variance factor for the full model is estimated. Applying these two steps results in the a-posteriori vc matrix.

3.4. Functional model

Besides the stochastic model, the functional model has to specified. In this section functional models to validate the InSAR double-differences with the leveling measurements are described. Examples are shown from models of condition and observation equations and a combination of the two.

3.4.1. Model of condition equations

The model of condition equations [11] in its most simplified form is based on the idea that the InSAR double-differences should be equal to the leveling double-differences. It reads:

$$B^* E\{\underline{y}\} = \begin{bmatrix} -I & I & 0 \\ -I & 0 & I \end{bmatrix} \begin{bmatrix} \underline{dd}_{\mathrm{Lev}} \\ \underline{\varphi}_{\mathrm{E2}} \\ \underline{\varphi}_{\mathrm{ES}} \end{bmatrix}_{\substack{\Delta t \\ \Delta cr}} = 0 \tag{16}$$

$$P_A^{\perp} = P_{Q_y B} = Q_y B (B^* Q_y B)^{-1} B^* \tag{17}$$

where

B	condition equation designmatrix,
$\underline{y}$	vector of observables,
I	identity matrix,
$\underline{dd}_{\mathrm{Lev}}$	leveling double-difference observation,
$\underline{\varphi}$	InSAR double-difference observation,
Δcr	spatial difference wrt. reference cr ($cr - cr_{ref}$),
Δt	time difference wrt. master scene ($t_m - t_s$).

This model cannot be extended adding equations conditioning that InSAR ERS-2 and Envisat double-differences should be equal, as this would result in a singular problem as the B matrix would not be of full rank due to dependent columns.

3.4.2. Alternative hypothesis - mixed model

If the misclosures of the InSAR-leveling double-differences indicate the presence of systematic effects, the functional model was possibly too idealized. To test the significance of the misclosures, alternative hypotheses have to be specified and therefore it is necessary to define physical causes which lead to the misclosures. An example of such a physical cause is sagging of the corner reflector's blades in time. This results in a deviating offset between the leveling and InSAR double differences, independent of the SAR sensor. Looking at Fig. 10, this effect is possibly present in the time series of corner reflector 5.

A way to test the presence of the sagging effect, is to set up a mixed model in which sagging parameters can be estimated. For linear sagging, this model reads:

$$B^* E\{\underline{y}\} = Ax \tag{18}$$

$$\begin{bmatrix} -I & I & 0 \\ -I & 0 & I \end{bmatrix} \begin{bmatrix} \underline{dd}_{\mathrm{Lev}\,\Delta cr}^{\Delta t} \\ \underline{\varphi}_{\mathrm{E2}\,\Delta cr}^{\Delta t} \\ \underline{\varphi}_{\mathrm{ES}\,\Delta cr}^{\Delta t} \end{bmatrix} = [B_T]\,[sag_{\Delta cr}] \tag{19}$$

where

A	observation equation designmatrix,
x	vector of unknown parameters,
B_T	diagonal matrix of temporal baselines,
$sag_{\Delta cr}$	sagging velocity relative to reference cr.

The vector of linear sagging parameters in mm/day per corner reflector is represented by sag. The significance of the estimated sagging parameters can be evaluated using the v-teststatistic [12]:

$$\underline{v} = \frac{\hat{\underline{x}}}{\sigma_{\hat{\underline{x}}}} \qquad \text{reject } H_0 \text{ if } v > k_\alpha \tag{20}$$

where

$\hat{\underline{x}}$	unknown parameter estimate,
$\sigma_{\hat{\underline{x}}}$	standard deviation of unknown parameter,
k_α	critical value for level of significance α.

First tests for estimation of sagging parameters show that they are around -0.02 mm/day for corner reflector 5. As their standard deviation is around 0.02 mm/day, they do not seem to be significant. The fact that all observations are spatial differences relative to a reference corner reflector complicates the interpretation of the estimated sagging parameters.

3.4.3. Model of observation equations

The model of observation equations is defined in [2]. The advantage of using this model, compared to the simplified model of condition equations, is the split up of the InSAR double-difference observable into deformation and height components. In this way, additional physical information is included in the functional model, leading to a higher redundancy in this case. The model reads:

$$E\{\underline{y}\} = Ax \tag{21}$$

$$E\{\begin{bmatrix} \underline{\varphi}_{\mathrm{E2}\,\Delta cr}^{\Delta t} \\ \underline{\varphi}_{\mathrm{ES}\,\Delta cr}^{\Delta t} \\ \underline{dd}_{\mathrm{Lev}\,\Delta cr}^{\Delta t} \\ \underline{h}_{\mathrm{gps}} \end{bmatrix}\} = \begin{bmatrix} k_{1\mathrm{E2}} & k_{2\mathrm{E2}} \\ k_{1\mathrm{ES}} & k_{2\mathrm{ES}} \\ I & 0 \\ 0 & I \end{bmatrix} \begin{bmatrix} D \\ H \end{bmatrix} \tag{22}$$

$$P_A^\perp = I - A(A^* Q_y^{-1} A)^{-1} A^* Q_y^{-1} \tag{23}$$

where

φ	InSAR double-difference (cycles),
dd_{Lev}	leveling double-difference (mm, LOS),
h_{gps}	corner reflector GPS heights (mm),
k_1	$2\lambda^{-1}$,
k_2	$k_1 B_\perp sin^{-1} R^{-1}$,
D	double-difference deformation in LOS (mm),
H	topographic height difference wrt. cr_{ref} (mm).

As the InSAR observations are unwrapped to the closest leveling observation, ambiguities should be estimated for the match between ERS-2 and Envisat double-differences. However, including estimation of the ambiguities would significantly reduce the redundancy and therefore result in less reliable estimates of the three variance components. As only very few double-differences would change when unwrapping to the closest match between the two types of InSAR double-differences, this has been left out for now.

3.4.4. Results from Variance Component Estimation

VCE has been performed for the model of observation equations according to [2]. First two variance factors for ERS-2 and Envisat have been estimated, subsequently one variance factor for the entire model. The results are shown in Fig. 11. The mean double-difference standard deviation is 4.4 mm for Envisat and 5.4 mm for ERS-2. Applying the propagation law for point scatterers backwards this would lead to standard deviations of 3.1 mm and 3.9 mm for respectively Envisat and ERS-2 single InSAR phase measurements (mm along the vertical).

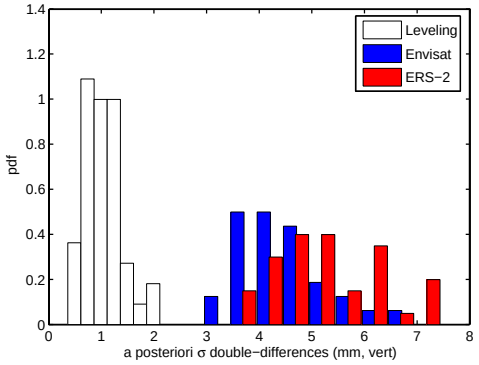

Figure 11. Model of observation equations: estimated double-difference standard deviation for Leveling, ERS-2 and Envisat.

The corner reflector phase variances based on SCR

are overestimated. It would therefore be recommendable to use the SCR based on maximum clutter for estimating the a-priori phase variances. The a-posteriori standard deviation for ERS-2 is higher than for Envisat. This may be caused by the large Doppler shifts for ERS-2, although there is no conclusive evidence for that. Further investigation of the adjustment residuals may reveal systematic effects which are not modeled in the functional model. In this case, alternative hypotheses have to be specified and tested. The a-posteriori leveling double-difference standard deviation is around 1 mm.

4. CONCLUSIONS

SCR estimates in SAR images can be used to obtain a-priori phase variances for point scatterers like the corner reflectors. Only for point scatterers with a phase standard deviation lower than 0.25 rad, phase residuals can be assumed normally distributed and the SCR phase variance estimate unbiased. The SCR's for the five corner reflectors have both been estimated using minimum and maximum clutter. In case of maximum clutter, the estimated phase variance for the corner reflectors is around 0.4 mm, both for ERS-2 and Envisat. As they appear to be time independent, one SCR estimate per corner reflector should be sufficient to serve as a-priori phase variance in the full time series. However, this time dependency is likely to be influenced by the SCR and the type of surroundings.

Leveling measurements have been introduced as an independent technique with well-known observation statistics, to validate the InSAR phase statistics. As in case of InSAR the first information-bearing variates are the double-differences, this type of observation is used for comparison. The InSAR-leveling double-difference comparison shows larger deviations for ERS-2 than for Envisat. The cause of this may be found in the processing chain, as the correction for subpixel position within the resolution cell of the corner reflectors needs to be improved for large Doppler shifts and baselines. For corner reflector 5, a deviating behavior for both ERS-2 and Envisat from the leveling double-differences is visible. This may suggest physical causes, like sagging of the blades.

A-posteriori variance factors for both ERS-2 and Envisat double-differences have been estimated using Variance Component Estimation in the Delft adjustment and testing theory. The results shows an overestimation of the a-priori SCR phase variance. It is therefore to be recommended to use maximum clutter for the SCR estimates. The estimated InSAR phase standard deviations are 3.1 mm for Envisat and 3.9 mm for ERS-2 (mm, vertical). This is higher than to be expected for a point target like a corner reflector.

REFERENCES

[1] Ferretti A., Prati C., and Rocca F., "Permanent scatterers in SAR interferometry," *IEEE Transactions on Geoscience and Remote Sensing*, vol. 39, no. 1, pp. 8–20, Jan. 2001.

[2] Hanssen R., "Stochastic modeling of time series radar interferometry," in *International Geoscience and Remote Sensing Symposium, Anchorage, Alaska, 20–24 September 2004*, 2004, pp. cdrom, 4 pages.

[3] Colesanti C., Ferretti A., Novali F., Prati C., and Rocca F., "SAR monitoring of progressive and seasonal ground deformation using the Permanent Scatterers Technique," *IEEE Transactions on Geoscience and Remote Sensing*, vol. 41, no. 7, pp. 1685–1701, July 2003.

[4] Kampes B. M., and Hanssen R. F., "Ambiguity resolution for permanent scatterer interferometry," *IEEE Transactions on Geoscience and Remote Sensing*, vol. in print, 2004.

[5] Teunissen P. J. G., de Jonge P. J., and Tiberius C. C. J. M., "A new way to fix carrier-phase ambiguities," *GPS World*, pp. 58–61, Apr. 1995.

[6] Just D., and Bamler R., "Phase statistics of interferograms with applications to synthetic aperture radar," *Applied Optics*, vol. 33, no. 20, pp. 4361–4368, 1994.

[7] Marinkovic P., Ketelaar G., and Hanssen R., "A controled Envisat/ERS permanent scatterer experiment, implications of corner reflector monitoring," in *CEOS SAR Workshop, Ulm Germany, 27–28 May 2004*, 2004, p. submitted.

[8] Xia Y., Kaufmann H., and Guo X., "Differential SAR interferometry using corner reflectors," in *International Geoscience and Remote Sensing Symposium, Toronto, Canada, 24–28 June 2002*, 2002.

[9] in *CEOS SAR Calibration Workshop, ESTEC, Noordwijk, The Netherlands, 20-24 Sept 1993*, 1993.

[10] Tiberius C. C. J. M., and Kenselaar F., "Variance component estimation and precise gps positioning: case study," *Journal of Surveying Engineering*.

[11] Teunissen P. J. G., *Adjustment theory; an introduction*, 1st ed. Delft: Delft University Press, 2000.

[12] ——, *Testing theory; an introduction*, 1st ed. Delft: Delft University Press, 2000.